Remnant Magnetization Behavior of a K-Doped Ba122 Polycrystalline Bulk

Fumitake Kametani, *Member, IEEE*, Shah Alam Limon, Keyou Mao, Eric Hellstrom, *Senior Member, IEEE*, and Chiara Tarantini, *Senior Member, IEEE*

(Invited Paper)

***Abstract*—It is still largely elusive whether K-doped $BaFe_2As_2$ (K-Ba122) is granular due to the intrinsic blocking effects at the grain boundaries (GBs). We investigated the remnant magnetization characteristics of a K-Ba122 polycrystalline bulk. Remnant magnetization is effective to evaluate the contribution of magnetization from multi-scale current loops particularly if electromagnetic granularity is present due to weakly coupled GBs. The derivative of remnant magnetization of the K-Ba122 sample showed only a single peak, which was markedly dependent on the specimen size and shifted toward lower field as the specimen size decreases, strongly indicating that the current loop is intergrain. However, the high angle annular dark field scanning transmission electron microscope (HAADF-STEM) analysis revealed that this sample still has nano-cracks at GBs, degrading the continuous network of strong intergrain connectivity. Such extrinsically degraded network of intergrain connectivity can also be seen as a size-dependence of remnant magnetization J_c, which indicated the presence of strongly localized regions with much higher J_c than the bulk J_c. Our study suggested that the extrinsic GB nano-cracks are still the major cause of connectivity degradation, and the intrinsic current suppression might not be practically detectable at clean, fully connected GBs.**

***Index Terms*—Critical current density, Fe-based superconductors, intergrain connectivity, K-doped Ba122, remnant magnetization.**

I. Introduction

In order to transform the Fe-based superconductor (FBS) K-doped $BaFe_2As_2$ (K-Ba122) into a truly magnet-ready high field conductor, there are several scientific and technological hurdles to overcome. As the most versatile form of superconductors is a long-length wire in which the materials are inevitably polycrystalline, J_c across the grain boundary (GB) network, the so-called intergrain J_c, must be raised to the practical level (J_c(4.2 K, 10 T) $> 10^3$ A/mm^2 in kilometer length wires). To this date, the critical current density J_c of polycrystalline or uniaxially textured K-Ba122 is still noticeably below the intrinsic intragrain properties even considering the very recent progress of J_c in the tape forms [1], [2], [3], [4], [5], [6], [7], [8], [9]. The important question for evaluating the potential of K-Ba122 is whether the GBs intrinsically block the current or are extrinsically degraded due to microstructural defects. Recent studies suggested that the intergrain connectivity of K-Ba122 is highly vulnerable to extrinsic microstructural factors such as local or global impurity segregations and GB cracks [10], [11], as well as oxygen contamination which easily degrades GB connectivity [11], [12]. Our previous comparison of the grain and GB nanostructures in two K-Ba122 tapes with similar J_c also revealed that the macroscopic tape J_c is actually derived from the complex combination of the quality of GB connectivity and the number of strongly connected GB networks. The former was strengthened by the grain alignment and the latter was enhanced by the clean GB nanostructure without FeAs or BaO blockage [10]. Thus, it is still largely unknown whether the J_c of polycrystalline K-Ba122 is limited by the intrinsic GB characteristics.

A previous study by Yamamoto et al. showed that remnant magnetization is very effective to distinguish the contribution to magnetization J_c from the intergrain connectivity and the individual grains, especially when the sample is highly electromagnetically-granular due to the intrinsic GB blockage [13], for instance due to local suppression of the superfluid density, reduced transparence caused by short coherence length, or high anisotropy. Here we utilized the remnant magnetization characterization to investigate the extrinsic and intrinsic connectivity in a K-Ba122 bulk whose J_c is equivalent to the best we reported [6]. The derivative of remnant magnetization and analysis of remnant magnetization J_c strongly suggested that the magnetization J_c of this K-Ba122 is derived only from intergrain connectivity, and no feature can be associated to an intragrain contribution. Our results revealed that there are strongly connected current paths but sub-divided by GB nano-cracks into

Received 26 September 2024; revised 21 November 2024; accepted 4 December 2024. Date of publication 16 December 2024; date of current version 31 December 2024. This work was supported in part by the U.S. Department of Energy, Office of Science, and Office of High Energy Physics under Grant DE-SC0018750, in part by the National High Magnetic Field Laboratory through the National Science Foundation under Grant NSF/DMR- 2128556, and in part by the State of Florida. *(Corresponding author: Fumitake Kametani.)*

Fumitake Kametani and Eric Hellstrom are with Applied Superconductivity Center, National High Magnetic Field Laboratory, Florida State University, Tallahassee, FL 32312 USA, and also with the Department of Mechanical Engineering, FAMU-FSU College of Engineering, Florida State University, Tallahassee, FL 32310 USA (e-mail: kametani@asc.magnet.fsu.edu; hellstrom@asc.magnet.fsu.edu).

Shah Alam Limon, Keyou Mao, and Chiara Tarantini are with Applied Superconductivity Center, National High Magnetic Field Laboratory, Florida State University, Tallahassee, FL 32310 USA (e-mail: slimon@fsu.edu; smao@eng.famu.fsu.edu; tarantini@asc.magnet.fsu.edu).

Color versions of one or more figures in this article are available at https://doi.org/10.1109/TASC.2024.3519074.

Digital Object Identifier 10.1109/TASC.2024.3519074

multi-scale domains whose size is much smaller than the entire bulk.

II. Experimental

A polycrystalline K-Ba122 bulk was synthesized from elemental starting materials with the nominal composition of $(Ba_{0.6}K_{0.4})Fe_2As_2$. The elemental materials were mixed in a Fritsch P7 Premium planetary high energy ball miller with the milling energy density E_{BM} of 100 MJ/kg. The milled powder was heat treated at 750 °C for 10 hours, then milled again, followed by the 2nd heat treatment at 600 °C for 10 hours in an AIP Hot Isostatic Press (HIP). The details of synthesis procedure can be found in [6] with the only difference that here the first heat treatment was performed at ambient pressure. The definition of E_{BM} can be found in [14], [15]. Magnetization J_c was measured by field-dependent magnetization hysteresis loops in a Quantum Design 16T-PPMS Vibrating Sample Magnetometer (VSM) on a sample with a cross-section of 1×2.65 mm^2 and a thickness of 1 mm parallel to the field. We used the SI-units Bean formula $J_c = 2\Delta M/(w \times (1\text{-}w/(3l)))$. Other magnetization measurements were performed in a Quantum Design SQUID Magnetometer MPMS XL5. Remnant magnetization was measured in bulk form first with the field parallel to the longest edge (sample sizes $2.39 \times 1.58 \times 1.50$ mm^3). Then the bulk was crushed into smaller pieces and then ground into powders performing remnant magnetization measurements in all cases. Nanostructural observations were carried out using a JEOL ARM200cF scanning transmission electron microscope (S/TEM).

III. Results

The temperature dependence of magnetization at 2 mT in the zero-field-cooled (ZFC) state of the K-Ba122 bulk is shown in Fig. 1(a). Magnetic onset, T_c, is 34.6 K, approximately 3 K lower than the optimally doped single crystal [2] that is typical for the high J_c K-Ba122 bulks [6], [7]. The superconducting transition is quite sharp, implying good homogeneity and the bulk-scale shielding current in the sample. Fig. 1(b) represents magnetization J_c at 4.2 K as a function of applied field that is actually one of the highest among the reported K-Ba122 bulk samples. J_c is $\sim 2.2 \times 10^5$ A/cm^2 at self-field, slowly decaying to $\sim 7.9 \times 10^4$ A/cm^2, $\sim 2.2 \times 10^4$ A/cm^2 and then 1.7×10^4 A/cm^2 at 1 T, 5 T and 10 T, respectively.

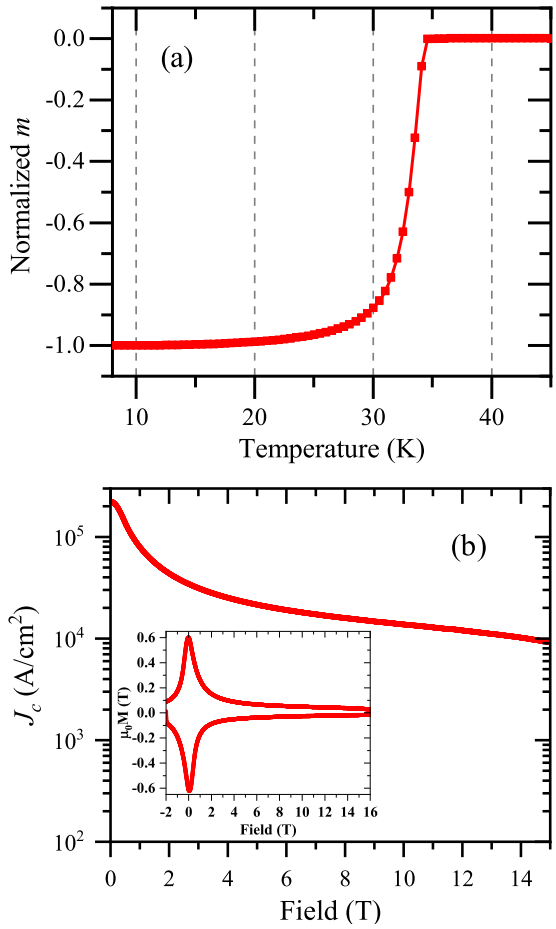

Fig. 1. (a) Temperature dependence of magnetization under zero-field-cooling (ZFC) at 2 mT. (b) Magnetization J_c (H) plot at 4.2 K; in the inset the hysteresis loop is shown.

Fig. 2(a) shows the remnant magnetization, m_R, as a function of increasing maximum field for the K-Ba122 bulk, crushed pieces and ground powder. For the bulk specimen, m_R starts to rise at $\sim$30 mT, sharply increasing and then saturating at $\sim$1–2 T. Unlike the other FBS bulks such as $SmFeAsO_{0.85}$ [13], a "shoulder" is not observed in m_R. As seen in Fig. 2(a), the crushed pieces and ground powder showed a similar m_R trend, although the m_R starts rising at a lower field ($\sim$13 mT and $\sim$4 mT, respectively) due to the smaller specimen size (because the field of first penetration should be proportional to $H_p \sim J_{c,global} \times$ sample size [13]). Indeed, only a single peak appears in the derivative of m_R in Fig. 2(b) regardless of the specimen size. As the specimen size decreases from the bulk, crushed pieces to powder, the peak of the m_R derivative shifted toward lower field, but it never separates into multiple peaks. This size dependence of the m_R derivative suggests that the magnetization current loop is also size-dependent thus the magnetization J_c is determined solely by the intergrain connectivity.

The intergrain J_c was calculated from the peak positions in the m_R derivative with the typical formula $J_{c,global} = 2H_{peak}/w$ (in crashed and powdered sample w was an average of the piece/particle sizes) [13] and plotted as a function of temperature (Fig. 3) and it is size-dependent. If the GB connectivity was uniform (no matter how good or bad the average connectivity is), J_c obtained by m_R should be independent of the sample size (i.e., bulk, crushed pieces, and powder). However, this K-Ba122 sample shows different J_c values for different sizes. J_c appears to increase going from the bulk to the crushed pieces, then to the powder specimen. The remnant magnetization J_c of the ground powder appears more than 2.5 times than that of the bulk specimen, although those powders originate from the same bulk sample. This apparent contradiction indicates that the bulk sample is already segmented into domains smaller than the whole sample and those domains have a higher J_c than that estimated at the macroscopic scale.

Fig. 4 is a TEM image of grain structure in the K-Ba122 sample. The grains are mostly equiaxed and randomly oriented.

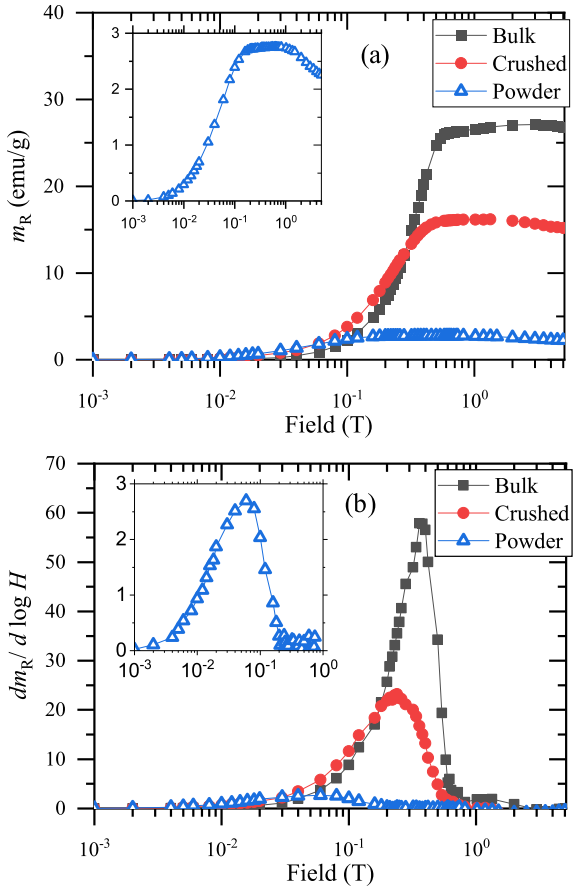

Fig. 2. (a) Remnant magnetization (m_R) as a function of the maximum field applied at 5 K for the bulk, crushed pieces and ground powder specimen. (b) Derivatives of m_R at 5 K.

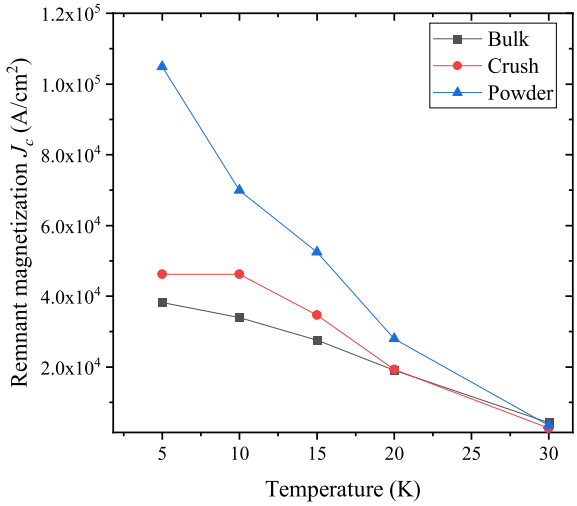

Fig. 3. Size dependence of the intergrain J_c as a function of temperature derived from the peak position of the remnant magnetization, strongly indicating that the strongly connected high J_c regions are highly localized.

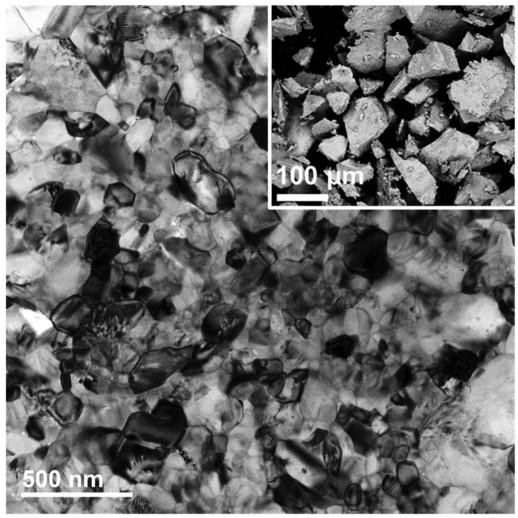

Fig. 4. TEM micrograph showing the grain structure in the K-Ba122 bulk sample. The grains are randomly oriented, and the average grain size is ~100 nm. (Inset) SEM image showing the ground powder specimen from the same bulk. The average powder particle size is ~90 μm.

The average grain size is estimated in 105 ± 17 nm. It is important to note that the average size of the ground powder particles is 91 ± 58 μm, as seen in the SEM micrograph inset in Fig. 4, which is far larger than the average grain size. This confirms that the higher J_c of the ground powder in Fig. 3 is still intergrain J_c, not J_c of a single grain, implying that the high-J_c loop is on the scale of large multigrain domains with strong GB connectivity.

HAADF-STEM imaging revealed the highly probable root cause of such segmentation of high-J_c loop. The Z-contrast image of Fig. 5(a) showed dark contrast traces on portions of GBs. As the brightness of Z-contrast is proportional to the local atomic density, such dark traces of GBs indicate either local compositional or atomic density variation. As shown in Fig. 5(b), the energy dispersive spectroscopy (EDS) line scan across the two dark Z-contrast GBs in Fig. 5(a) showed almost no variation of As, Fe, K, or Ba, indicating that the dark traces of GBs are caused by local lower density, so-called nano-cracks. Indeed, we also found extensive distribution of GB nano-cracks even in the highest J_c bulk sample in our previous study on K-Ba122 synthesis [6].

IV. Discussion

In the case of fully granular superconductor bulks such as $SmFeAsO_{0.85}$ (the other so-called 1111 FBS material), the grains were very weakly coupled, resulting in a clear separation of intragrain and intergrain contributions to remnant magnetization, for which the two peaks appear in the m_R derivatives as demonstrated by Yamamoto et al. [13]. For such a case, the intergrain contribution of weak GB connectivity causes the low-field peak to be suppressed and shifted to lower field as the sample size decreases. On the contrary the intragrain contribution appears as the high-field peak remaining at the same field because the intragrain current loop is unaffected by changing the specimen macroscopic size. Thus, the analysis of remnant magnetization can provide information about the degree of superconducting granularity and whether the GB connectivity is intrinsically weak or not.

Differently, in our K-Ba122 bulk sample, the m_R derivative showed only a single peak whose position shifts to lower field as the specimen size decreases, strongly indicating that the current

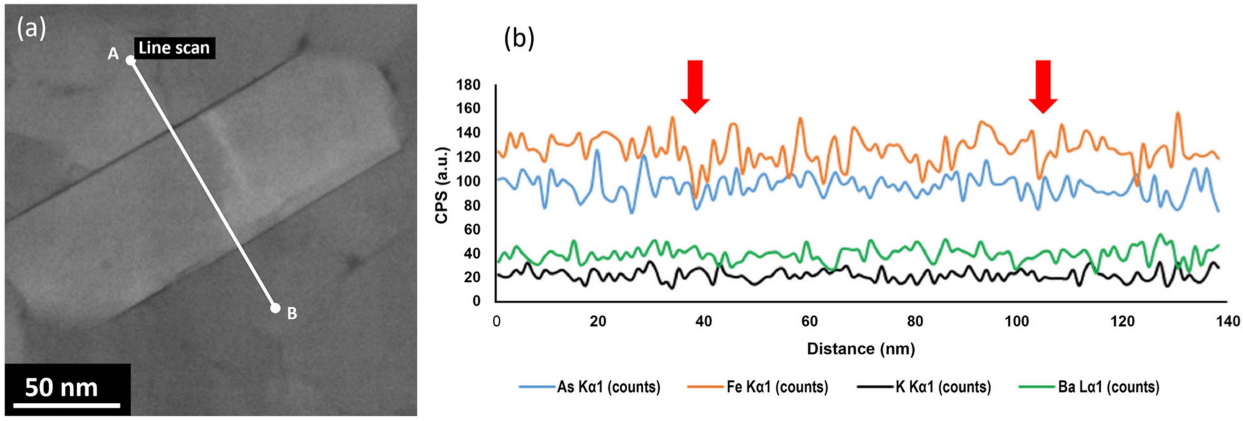

Fig. 5. (a) HAADF-STEM image showing the GB nanostructure. The dark contrast traces indicate the low-density region at the GBs. (b) EDS line scans from point A to point B in (a) showing no compositional variation of As, Fe, K and Ba across the GBs. The red arrows show the locations of GBs.

loop is size-dependent, thus remnant magnetization is derived only by the intergrain current. Correlations of a single peak to the intergrain contribution was also found in [16]. There are two possible reasons for why the intragrain component is invisible. One is that the GBs are strongly coupled and not intrinsically blocking current. The other is that the grains are so small that the magnetization of single grains is undetectable [17]. The London penetration depth of K-Ba122 is reported to be approximately 200 nm [18], which is larger than the average grain size of this sample. It appears possible that the external field penetrates through the GBs and inside the grains almost simultaneously so that the intragrain and intergrain contribution to magnetization cannot be separated. However, our remnant magnetization measurements did not show evidence of intrinsic GB blockage. Although some current limiting effects were observed in [001]-tilt bicrystal films [19], this is not necessarily relevant to bulk samples in which GBs are largely meandering and have a much more complex geometrical nature, compared with the almost ideal straight GB on bicrystal films. In fact, even in films of the higher anisotropic YBCO, meandering GBs are not particularly detrimental to J_c [20], and also in FBS even straight GBs do not suffer from current limiting effect when the field is not parallel to the GB, so preventing vortex channeling [21]. Our results of the bulk samples suggest that the grains are mostly strongly coupled when they are physically strongly connected.

However, the remnant magnetization J_c analysis also suggested that the GB connectivity is still highly variable in the K-Ba122 sample. As briefly stated earlier, the remnant magnetization J_c should be size-independent if the GB connectivity is uniform on the scale of the entire bulk. As shown in Fig. 3, strong size-dependence appears in the remnant magnetization J_c, which increases 2.5 times in the ground powder. This J_c increment indicates that the size of strongly connected high-J_c regions is smaller from the beginning than the size of the bulk, and that the macroscopic bulk J_c is determined by complex combinations of multiple scales of current loop including such high-J_c regions and the J_c between those regions. Unlike old bulk samples whose GBs were highly degraded by the impurity phases of FeAs and BaO, this bulk did not show such a compositional degradation at GBs (Fig. 5(b)). However, HAADF-STEM revealed nano-cracks at the GBs (Fig. 5) whose networks disconnect a fraction of GBs and presumably locally decouple the high-J_c regions or produce an effective reduction of the current cross-section. This study of remnant magnetization and GB nanostructure indicates that the macroscopic bulk J_c can be largely increased if the high-J_c region can be formed continuously at the macroscopic scale.

V. Conclusion

Remnant magnetization analysis was performed in order to investigate the intragrain and intergrain contribution to magnetization J_c of the K-Ba122 polycrystalline bulk. Strikingly, the K-Ba122 bulk sample does not show clear intragrain/intergrain peak separation in the derivative of m_R. In fact, the peak of the m_R derivative shifts to lower field as the specimen size decreases from bulk, to crushed pieces then to powder, strongly indicating that the remnant magnetization is predominantly determined by the intergrain contribution. This implies that K-Ba122 has no visible electromagnetic granularity at the GBs. However, the apparent size-dependence of remnant magnetization J_c suggested that the magnetization J_c is determined by complex combinations of multi-scale current loops as a result of the GB nano-cracks locally decoupling the high-J_c regions.

References

[1] C. Tarantini et al., "Significant enhancement of upper critical fields by doping and strain in iron-based superconductors," *Phys. Rev. B*, vol. 84, no. 18, Nov. 2011, Art. no. 184522, doi: 10.1103/PhysRevB.84.184522.

[2] S. Ishida et al., "Doping-dependent critical current properties in K, Co, and P-doped $BaFe_2As_2$ single crystals," *Phys. Rev. B*, vol. 95, no. 1, Jan. 2017, Art. no. 014517, doi: 10.1103/PhysRevB.95.014517.

[3] H. Huang et al., "High transport current superconductivity in powder-in-tube $Ba_{0.6}K_{0.4}Fe_2As_2$ tapes at 27 T," *Supercond. Sci. Technol.*, vol. 31, no. 1, Jan. 2018, Art. no. 015017, doi: 10.1088/1361-6668/aa9912.

[4] Z. Gao, K. Togano, Y. Zhang, A. Matsumoto, A. Kikuchi, and H. Kumakura, "High transport J_c in stainless steel/Ag-Sn double sheathed Ba122 tapes," *Supercond. Sci. Technol.*, vol. 30, no. 9, Sep. 2017, Art. no. 095012, doi: 10.1088/1361-6668/aa7bb9.

[5] S. Pyon et al., "Enhancement of critical current densities in $(Ba,K)Fe_2As_2$ wires and tapes using HIP technique," *Supercond. Sci. Technol.*, vol. 29, no. 11, Nov. 2016, Art. no. 115002, doi: 10.1088/0953-2048/29/11/115002.

[6] C. Pak et al., "Synthesis routes to eliminate oxide impurity segregation and their influence on intergrain connectivity in K-doped $BaFe_2As_2$ polycrystalline bulks," *Supercond. Sci. Technol.*, vol. 33, no. 8, Aug. 2020, Art. no. 084010, doi: 10.1088/1361-6668/aba01a.

[7] J. D. Weiss et al., "High intergrain critical current density in fine-grain (Ba0.6K0.4)Fe_2As_2 wires and bulks," *Nat. Mater.*, vol. 11, no. 8, pp. 682–685, Aug. 2012, doi: 10.1038/nmat3333.

[8] E. Bellingeri et al., "Effects of K excess in microstructure of $(Ba_{0.6}K_{0.4})Fe_2As_2$ superconducting powders," *Supercond. Sci. Technol.*, vol. 37, no. 9, Sep. 2024, Art. no. 095014, doi: 10.1088/1361-6668/ad68d4.

[9] C. Dong et al., "Modulation of superconducting grain structure to achieve high critical current in $Ba_{0.6}K_{0.4}Fe_2As_2$ multifilament round wires," *J. Alloys Compounds*, vol. 932, Jan. 2023, Art. no. 167674, doi: 10.1016/j.jallcom.2022.167674.

[10] F. Kametani et al., "On the mechanisms of J_c increment and degradation in high-J_c Ba122 tapes made by different processing methods," *Appl. Phys. Exp.*, vol. 17, no. 1, Jan. 2024, Art. no. 013004, doi: 10.35848/1882-0786/ad1891.

[11] F. Kametani et al., "Chemically degraded grain boundaries in fine-grain $Ba_{0.6}K_{0.4}Fe_2As_2$ polycrystalline bulks," *Appl. Phys. Exp.*, vol. 13, no. 11, Nov. 2020, Art. no. 113002, doi: 10.35848/1882-0786/abbfdf.

[12] Y. -J. Kim, J. D. Weiss, E. E. Hellstrom, D. C. Larbalestier, and D. N. Seidman, "Evidence for composition variations and impurity segregation at grain boundaries in high current-density polycrystalline K- and Co-doped $BaFe_2As_2$ superconductors," *Appl. Phys. Lett.*, vol. 105, no. 16, Oct. 2014, Art. no. 162604, doi: 10.1063/1.4898191.

[13] A. Yamamoto et al., "Evidence for two distinct scales of current flow in polycrystalline Sm and Nd iron oxypnictides," *Supercond. Sci. Technol.*, vol. 21, no. 9, Sep. 2008, Art. no. 095008, doi: 10.1088/0953-2048/21/9/095008.

[14] W. Häßler et al., "Influence of the milling energy transferred to the precursor powder on the microstructure and the superconducting properties of MgB_2 wires," *Supercond. Sci. Technol.*, vol. 26, no. 2, Dec. 2012, Art. no. 025005, doi: 10.1088/0953-2048/26/2/025005.

[15] S. Tokuta and A. Yamamoto, "Enhanced upper critical field in Co-doped Ba122 superconductors by lattice defect tuning," *APL Mater.*, vol. 7, no. 11, Nov. 2019, Art. no. 111107, doi: 10.1063/1.5098057.

[16] S. Tokuta, Y. Shimada, and A. Yamamoto, "Evolution of intergranular microstructure and critical current properties of polycrystalline Co-doped $BaFe_2As_2$ through high-energy milling," *Supercond. Sci. Technol.*, vol. 33, no. 9, Sep. 2020, Art. no. 094010, doi: 10.1088/1361-6668/aba545.

[17] C. Tarantini, C. Pak, Y. -F. Su, E. E. Hellstrom, D. C. Larbalestier, and F. Kametani, "Effect of heat treatments on superconducting properties and connectivity in K-doped $BaFe_2As_2$," *Sci. Rep.*, vol. 11, no. 1, Feb. 2021, Art. no. 3143, doi: 10.1038/s41598-021-82325-x.

[18] S. Lee, Y. -S. Seo, S. Roh, D. Song, H. Eisaki, and J. Hwang, "Doping-dependent superconducting physical quantities of K-doped $BaFe_2As_2$ obtained through infrared spectroscopy," *Sci. Rep.*, vol. 12, no. 1, Nov. 2022, Art. no. 19950, doi: 10.1038/s41598-022-24520-y.

[19] T. Hatano et al., "High tolerance of the superconducting current to large grain boundary angles in potassium-doped $BaFe_2As_2$," *NPG Asia Mater.*, vol. 16, no. 1, Aug. 2024, Art. no. 41, doi: 10.1038/s41427-024-00561-9.

[20] D. M. Feldmann et al., "Mechanisms for enhanced supercurrent across meandered grain boundaries in high-temperature superconductors," *J. Appl. Phys.*, vol. 102, 2007, Art. no. 083912.

[21] J. H. Durrell et al., "The behavior of grain boundaries in the Fe-based superconductors," *Rep. Prog. Phys.*, vol. 74, no. 12, Dec. 2011, Art. no. 124511, doi: 10.1088/0034-4885/74/12/124511.